DOI: 10.5604/01.3001.0015.4796

Volume 108 • Issue 1 • September 2021

Journal of Achievements in Materials and Manufacturing Engineering

International Scientific Journal published monthly by the World Academy of Materials and Manufacturing Engineering

Effect of arc stud welding parameters on the microstructure and mechanical properties of AA6061 and AA5086 aluminium alloys

M.K.A. Razzaq *, A.N. Abood

Middle Technical University, Iraq

* Corresponding e-mail address: Mortadha_kareem@yahoo.com

ORCID identifier: https://orcid.org/0000-0002-9599-5359 (M.K.A.R.)

ABSTRACT

Purpose: This paper aims to investigate the effect of arc stud welding (ASW) process parameters on the microstructure and mechanical properties of AA6061-T6 and AA5086-H116 joint.

Design/methodology/approach: ASW process was done with argon as a shielding gas. Optical microscope (OM), scanning electron microscope (SEM), and X-Ray Diffraction (XRD) were employed to investigate the influence of welding current, welding time, and gas flow-rate on the microstructure of the fusion zone (FZ). Torque strength and Microhardness tests were used to evaluate the mechanical properties of the welded joints.

Findings: OM and SEM showed a cellular dendritic structure with equiaxed zone and columnar dendritic are forming at welding zone and weld interface. XRD analysis showed the precipitation of Mg_2Si and Al_3Mg_2 in the similar and dissimilar joints. Similar ASW of AA6061-T6/AA6061-T6 recorded 19 N·m torque strength, while dissimilar welding of AA6061-T6/AA5086-H116 registered 23 N·m. With increasing heat input, grains in Fusion Zone (FZ) and Heat Affected Zone (HAZ) coarsen and the hardness in both zones decreased. The hardness of similar weldments indicated a remarkable softening of FZ, while lower hardness values were registered in HAZ of dissimilar weldments. Softening of both weldments is due to the dissolution of the strengthening precipitates. Hot cracks exist with similar weldments, while no cracks evidence with dissimilar weldments.

Research limitations/implications: The main challenge in this work was how to minimize porosity level and how to avoid hot crack in the FZ.

Practical implications: The application of ASW with ceramic ferrule has an important role in different production areas such as; automobile industry, aircraft applications, and appliances industry.

Originality/value: Study the effect of welding current, welding time, and gas flow-rate of ASW process on microstructure and mechanical properties of AA6061-T6 and AA5086-H116 joint.

Keywords: Arc stud welding, Aluminium alloys, Solidification mode, Fusion zone, Mechanical properties

Reference to this paper should be given in the following way:
M.K.A. Razzaq, A.N. Abood, Effect of arc stud welding parameters on the microstructure and mechanical properties of AA6061 and AA5086 aluminium alloys, Journal of Achievements in Materials and Manufacturing Engineering 108/1 (2021) 24-34.
DOI: https://doi.org/10.5604/01.3001.0015.4796

1. Introduction

Prior to world war II**,** electric arc stud welding (ASW) was fabricated and advanced out of a necessity to fasten wood planking to naval aircraft carriers**.** Stud could be welding on the exterior side of steel deck plates by using only one welder rather than drilling holes through the plate. Since that time, stud using has increased exceedingly in construction industries and automotive [1-3]. ASW process involves the same mechanical, metallurgical, and electrical principles found in other arc welding processes [4]. Application of ASW with ceramic ferrule has an important role in different production areas such as; steam boiler production, bridge construction, shipbuilding, automobile industry and, appliances industry [5]. Inert shielding gas is used for ASW of aluminum with or without a ferrule. Because welding time is enough for oxidation to occur, so argon shielding should be used with the drawn arc method of aluminum [6]. Quality of joint depends on different welding variables, such as, stud material, type of base metal (BM), and welding position, but the selection of welding variables have an important role. Defects associated with a similar and dissimilar arc welding of aluminum alloys like gas porosity, hot tearing, lack of fusion, and excessive melting are due to the largest difference in solubility of hydrogen in liquid and solid aluminum, thermal conductivity, and chemical composition [7]. Furthermore, porosity may be caused by the interruption of dissolved gases on solidification and chemical reactions that generate gases in the molten weld puddle. Excessive hydrogen porosity can severely reduce the mechanical properties of aluminum welds [8]. Levels of porosity in the welds are dependent on welding procedures where both optimized gas shielding and pre-weld surface cleaning can be effective[9]. Other defects in arc welding of aluminum alloys are solidification cracks. For most investigated alloys, cracks were observed in the weld metal while heat affected zone (HAZ) was free from cracks. In aluminum alloys, weld cracking may be occur as a result of aluminum relatively wide solidification temperature range, a large change in volume upon solidification, and high thermal expansion. Aluminum alloys 5xxx and 6xxx series are known to be highly susceptible to the weld cracks in the arc welding processes [10,11]. S. Ramasamy [12] conducted a study to develop welding procedures for AA5754-O and AA6061-T6 alloys using a Drawn Arc Stud Welding (DASW). The results showed that DASW can be performed on AA5754-O and AA6061-T6 alloy sheets with matchmaking, good mechanical properties. It is the closest previous study for this manuscript, but it did not focus on the microstructure in details and did not study the variables that were investigated in this research. A. El-Batahgy, et al., [13] investigated Laser Beam Welding (LBW) of AA5083, AA5052, and AA6061 for sheets thickness of 2 and 3mm. From the results, all investigated alloys showed tendencies for solidification cracking and porosity. Hardness and tensile tests of AA6061 alloy weldments indicated a remarkable softening of the fusion zone (FZ) due to dissolution of the strengthening precipitates, while for AA5083 alloy, softening of FZ due to loss of its work-hardened condition was less in comparison with AA6061. Beytullah Gungor, et al., [14] investigated welding of AA5083-H111 and AA6082-T651 aluminum alloys using Pulsed Robotic Cold Metal Transfer-Metal Inert Gas technology. Joints were fabricated as both similar and dissimilar alloy welds using plates with a thickness of 6 mm. The results detected that this process provides good joint efficiency with high welding speed, and good tensile and fatigue performance.

The objectives of this investigation are to evaluate possibility of similar and dissimilar ASW joining for AA6061-T6 and AA5086-H116, studying the microstructure of FZ and HAZ of weldments, investigating the influence of ASW parameters on the Torque and Hardness of weldments, and evaluating the depth of penetration for similar and dissimilar weldments.

2. Experimental work

AA6061-T6 stud with 8 mm diameter and AA6061-T6 and AA5086-H116 plates with 6.4 mm thickness were used. Physical properties and chemical analysis of plate and stud are listed in Tables 1 and 2. Two different welding currents 200 and 400 A with welding times (0.1,0.2.0.3, 0.4, 0.5, 0.6 and 0.7 second) and four gas flow rates (15, 20, 25 and 30 L/min) were applied. The specimen for microstructure examination was prepared using grinding and polishing,

followed by etching with Keller's reagent. Microstructural features across BM, HAZ and FZ of the welded joint were examined by Optical microscope (OM) and scanning electron microscope (SEM). X-Ray Diffraction (XRD) analysis was used to investigate and identify phases at welded joints. Mechanical properties of welded joints were evaluated using torque and microhardness tests. Torque test was performed according to ISO 14555. Vickers hardness measurements were implemented using 200 g load and 15 second holding indentation time. Experimental work was done by using ASW machine type DABOTEK DT (1000) consists of a control unit, welding pistol, and argon chamber. Operation sequence for ASW process with ceramic ferrule is shown in Figure 1. Argon chamber was fabricated from commercial purity copper with specific dimensions to performance a good gas-protection, Figure 2.

Table 1.
Physical properties of AA6061-T6 and AA5086-H116 Aluminum alloys

Material	Thermal conductivity, W/m.K	Thermal expansion coefficient, $10^{-6}(°K)^{-1}$
AA6061-T6 BM	166	23.4
AA5086-H116 BM	121	25
AA6061-T6 Stud	166	23.4

Table 2.
Chemical Composition of AA6061-T6 and AA5086-H116 Plate and Stud

Element	Si%	Fe%	Cu%	Mn%	Mg%	Cr%	Zn%	Ti%	Al%
Wt.% AA6061-T6 BM	0.65	0.56	0.21	0.094	0.92	0.17	0.008	0.056	Bal.
Wt.% AA5086-H116 BM	0.35	0.40	0.06	0.5	4.30	0.18	0.14	0.08	Bal.
Wt.% AA6061-T6 Stud	0.68	0.62	0.32	0.11	1.1	0.21	0.09	0.08	Bal.

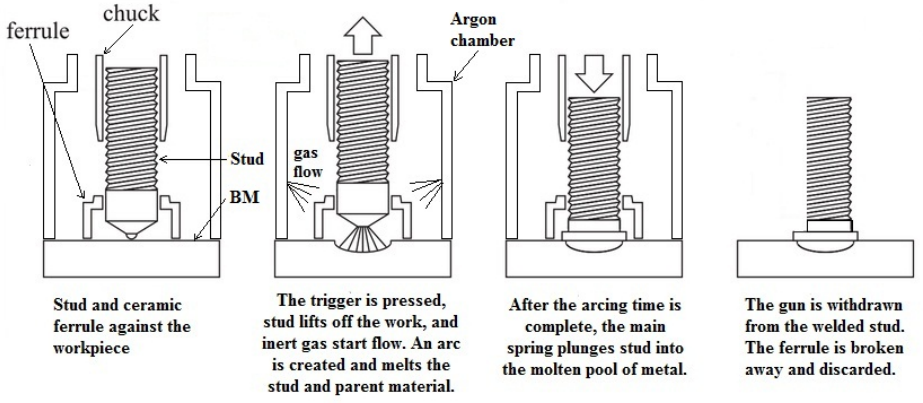

Fig. 1. Welding operation sequence for ASW with ceramic ferrule

Fig. 2. Stud welding gun with argon chamber

3. Results and discussion

3.1. Microstructure analysis

In FZ of similar weldments AA6061-T6/AA6061-T6, the weld metal formation primarily depending on solidification conditions like temperature gradient, solidification growth rate, and diffusion. Microscopy examination showed a cellular dendritic structure with equiaxed zone formation near the center of welding zone, as shown in Figure 3. Morphology of dendritic structure had been greatly affected by heat input. Fine dendritic is attributed to fast cooling rates in welding zone; this evident agreement with M. Temmar, et al. [15]. FZ microstructure has a dendritic feature, cellular dendrite, and equiaxed grains, while at the interface more columnar dendritic was predominant. This is related to the effect of thermal gradient (G) and growth rate (R) ratio [2]. At 200 A, 0.1 second, and 15 L/min, insufficient heat input lead to incomplete fillet with existing of a hot crack in the welding zone. Gas flow rate at 30 L/min gave good protection to welding zone. As a result, welding defects such as porosities were decreased.

Microstructure of AA6061-T6/AA5086-H116 is similar – to some extent – to AA6061-T6/AA6061-T6 for selected welding parameters Figure 4. Main differences are the width and depth of FZ. Behavior of dissimilar welded joints at 200 A, 0.2 second, 20 L/min is attributed to the migration of Mg from BM to FZ, resulting in an increasing amount of Mg_2Si and Al_3Mg_2 precipitates on dendritic boundary and aluminum matrix, that was detected by EDS Figure 5. When the temperature increased magnesium diffuses to the surface, resulting in formation of magnesium oxide (MgO). In dissimilar ASW, magnesium percentage at the welding zone will increase, due to fast cooling rate. So magnesium has not sufficient time to diffusion to surface. Somewhat, resemblance results were regarding at FZ for similar and dissimilar ASW.

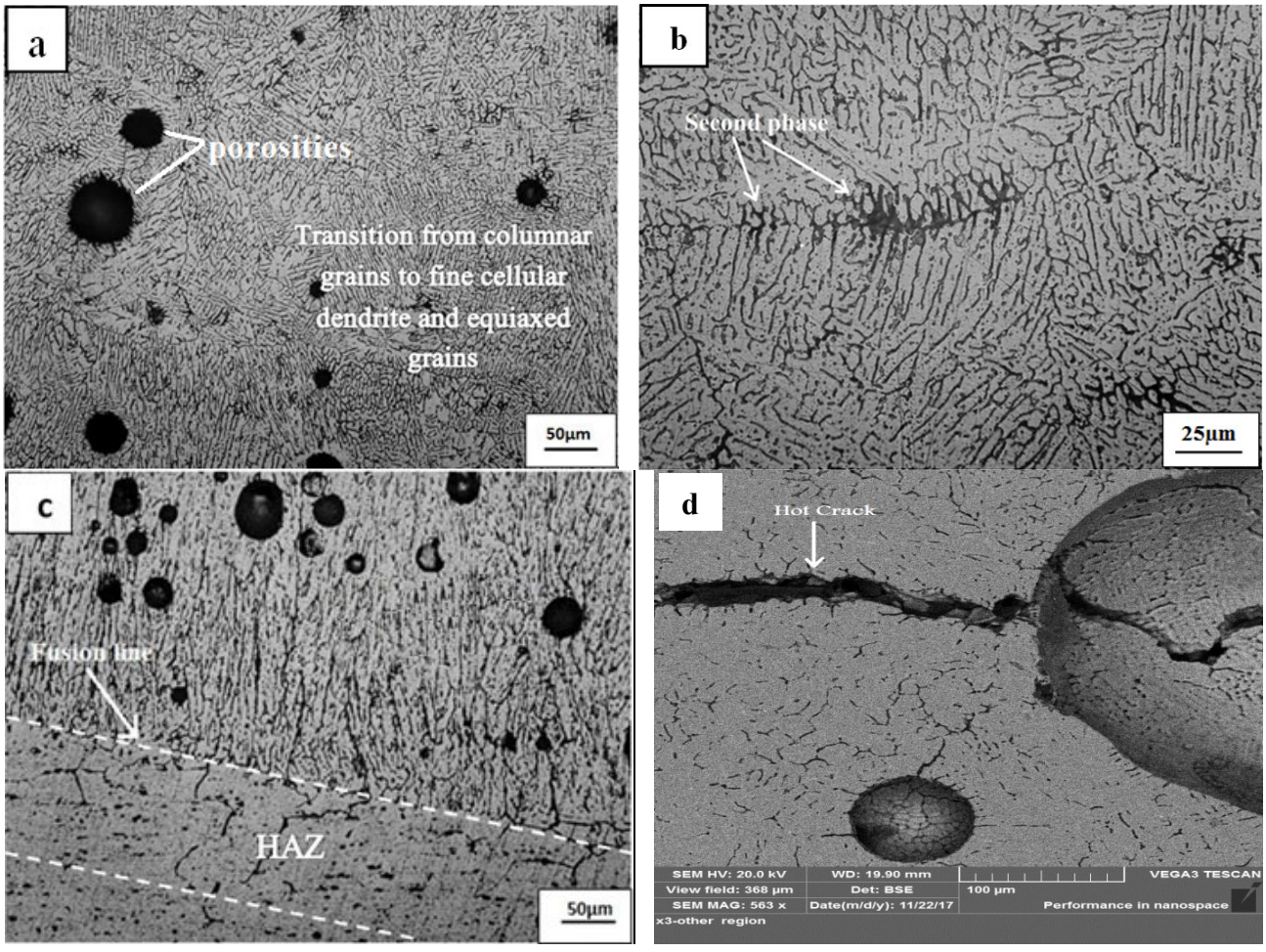

Fig. 3. Microstructure of similar weldment (a, b, and c) at 400 A, 0.2 second and, 30 L/min (d) at 200 A, 0.1 second, 15 L/min

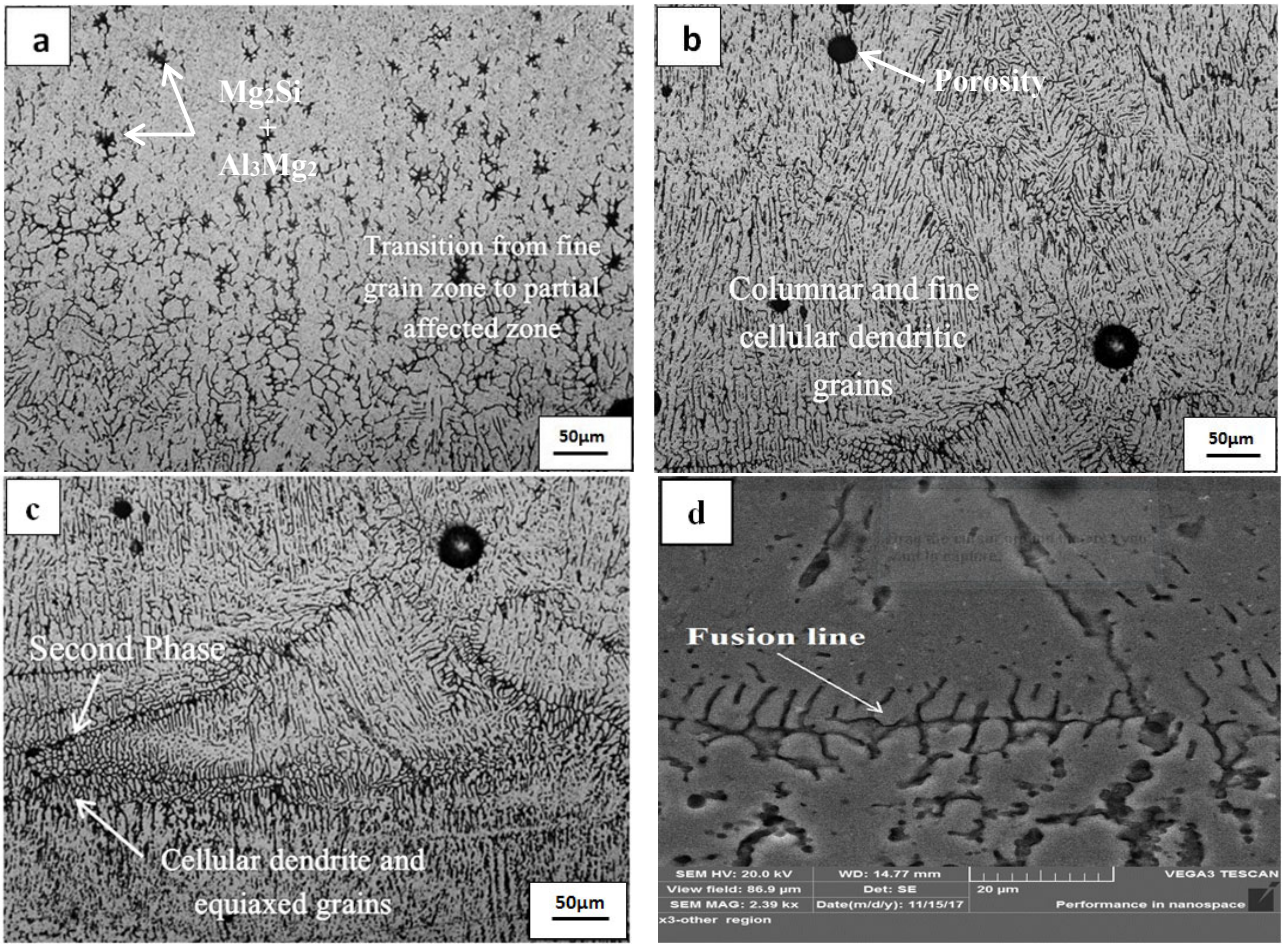

Fig. 4. Microstructure of dissimilar weldment at 200 A, 0.2 second, 20 L/min

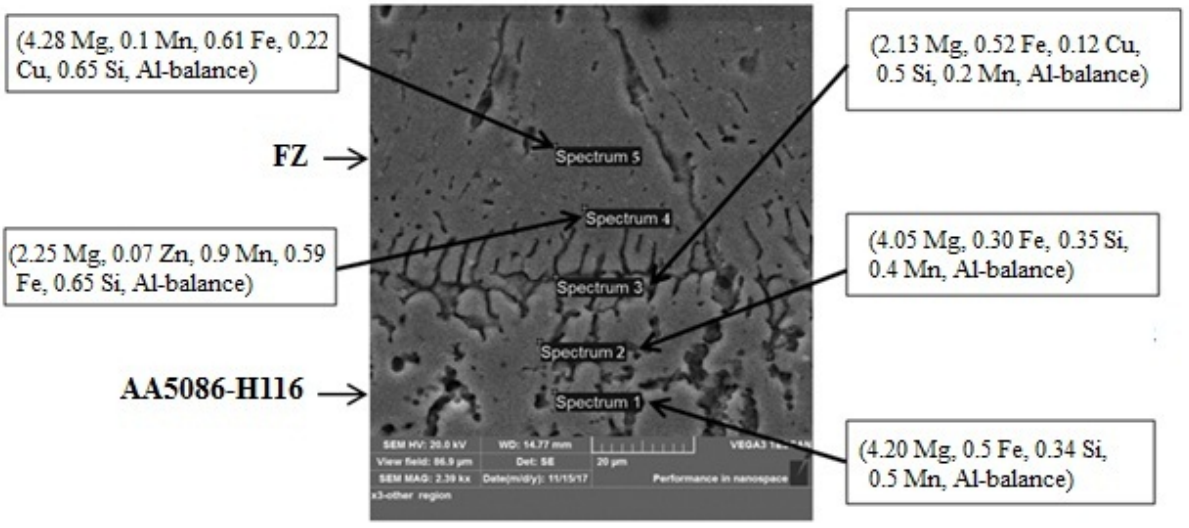

Fig. 5. AA6061-T6/AA5086-H116 joint, EDS results at 200 Amp, 0.2 second, 20 L/min

SEM examination showed that thermal characteristics of base metal affect depth of penetration. For dissimilar weldments, depth of penetration was equal to 2 mm approximately at 200 A, 0.3 second and, 15 L/min. While for similar ASW weldments, maximum depth was equal to approximately 1.25mm at 400 A, 0.2 second and, 30 L/min Figure 6. Depth of penetration of dissimilar is about 30% higher than that of similar ASW. This difference was attributed to high heat concentration of AA5086-H116 plate than AA6061-T6 plate, because of its lower thermal conductivity.

From XRD analysis (Figs. 7 and 8), it can be seen that α-Al is the main phase in all weldments, besides, two intermetallic compounds exist; Mg_2Si and Al_3Mg_2 in the FZ. They are precipitation strengthening phases, that commanded joint torque strength. FZ and HAZ were composed of fewer strengthening precipitates compared with the parent material. Low volume fraction of Mg_2Si and Al_3Mg_2 precipitated in the similar joints in view of dissolution of second phases. Due to diffusion of Mg from base metal AA5086-H116 towards welding zone, dissimilar weldments have high Mg_2Si and Al_3Mg_2 volume fraction in welding zone.

3.2. Mechanical properties

Torque strength

Minimum torque was recorded at 200 A, 0.1 second, and 15 L/min, due to existing high porosities level with hot cracks in welding zone, Figure 3d. Almost all heat-treatable aluminum alloys are prone to hot cracking and softening

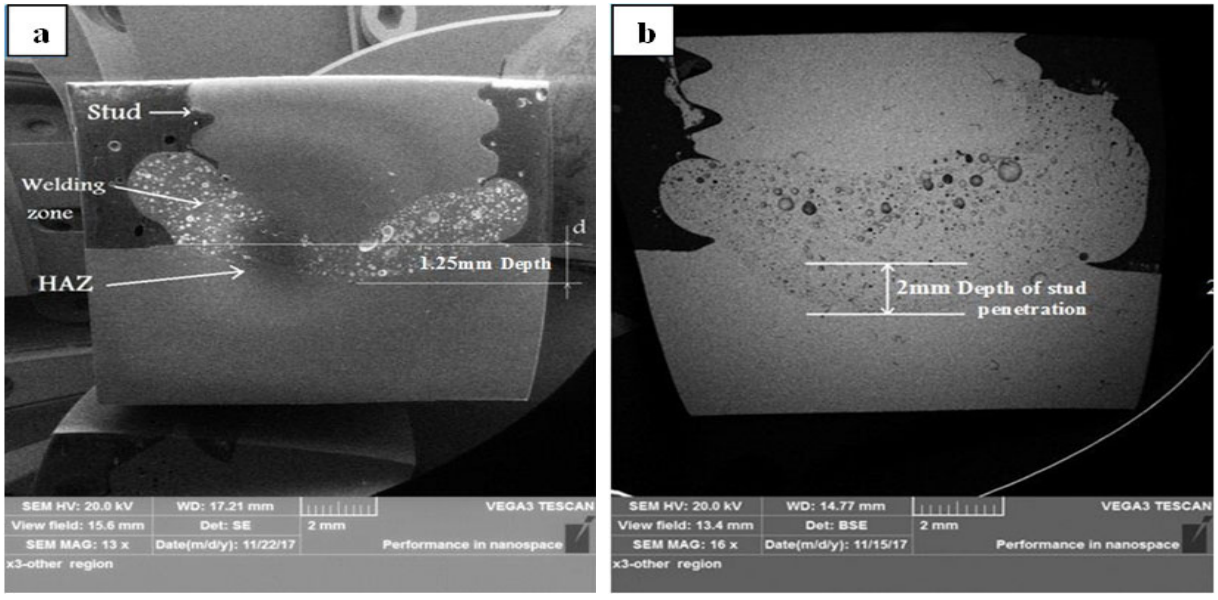

Fig. 6. SEM images of welded joints (a) penetration of similar weldment (b) penetration of dissimilar weldment

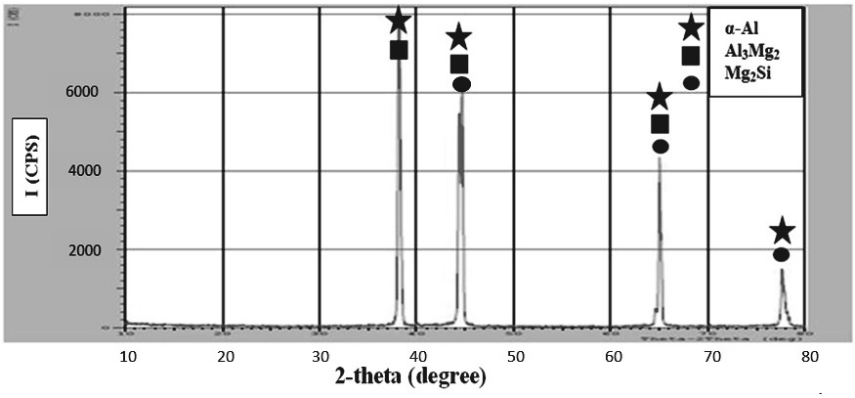

Fig. 7. XRD of AA6061-T6/AA6061-T6 weldment at 400 A, 0.2 second and 30 L/min

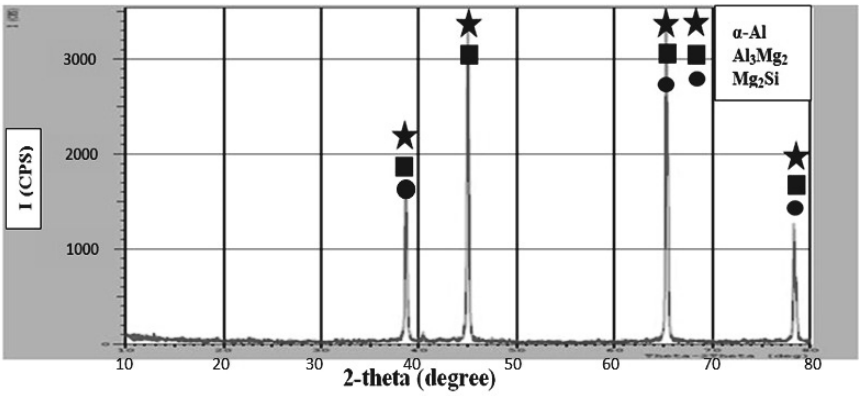

Fig. 8. XRD of AA6061-T6/AA5086-H116 weldment at 200 A, 0.2 second and 20 L/min

after arc welding [16]. Welding current has the greatest effect on mechanical properties. Higher welding current or larger welding time, encourage undercut defect and porosity formation in FZ, which reduce torque strength. At 400 A aluminum stud can be welded with 0.1, 0.2 and, 0.3 seconds as welding time, while welding did not occur at 0.4 second, owing to tremendous heat input that damage stud. At 200 A, an aluminum stud can be welded until 0.7 second. At 200 A, 15 L/min, and 0.1 second, torque strength is 6.84 N·m Figure 9, when increasing welding time up to 0.4 second with same current, this would give an increase in torque to 12.89 N·m. This is belongs to the fact that sufficient welding time provides a sufficient fillet around the stud with good weld penetration. While, further increment in welding time, results in declines in torque strength associated with excessive fusion at weld region. At 200 A, 0.1 second with lower gas flow rate (15 L/min), high porosity formation was observed in the weld region. Reduction in porosity was recognized when increasing gas flow rate to 30 L/min., which lead to enhancement in torque strength. Loss in the torque strength of aluminum welds is proportional to the loss of sound metal area in weld region. With 400 A, 0.2 second and 30 L/min, that was resulted in a maximum torque strength, a sound in weld region was the prevailing.

Minimum torque is registered at 200 A, 0.1 second, and 15 L/min, with a clear appearance of porosity in welding zone. So sufficient heat input and gas flow rate gave a homogenous weld and decreased macro and micro defects. At the same welding current and welding time (400 A, 0.2 second), increasing gas flow rate from 15 L/min to 30 L/min resulted in increasing torque strength from 14 N·m to 19 N·m, so the weldment torque was increased by 35%. Maximum torque is registered at 400 A, 0.2 second, and 30 L/min, corresponding with minimal level of visual defect and the failure take place within welding zone. Maximum recorded torque was exceeded minimum torque for 8 mm diameter aluminum stud, which is equal to 17 N·m.

For dissimilar weldment (AA6061-T6/AA5086-H116), current and time have a major effect in controlling torque. At 200 A, behavior of torque was found to raise gradually with time until arriving maximum value, then decreased. While, at 400 A, torque start with a maximum value at 0.1 sec. and then decreasing with increasing welding time Figure 10, this is a companion to excessive fusion with appearance of gas porosity at weld region. Increasing welding time and welding current over a certain limit leads to increasing probability of defect formation in the weld metal. This will affects on mechanical properties and soundness of welded metal, as mentioned by Che W. Mohd Noor [16].

Maximum torque of 23 N·m was recorded at 200 A, 0.2 second, 20 L/min and failure occurred within stud, away from welding zone. Under this situation welding zone was approximately free from porosities, while at worst condition (200 A, 0.7 second, 25 L/min), minimum torque strength was recorded and the porosities appeared. At 200 A and 0.2 second, increasing flow rate to 20 L/min at same welding current and time, torque strength increased to 23.47 N·m, then slightly decreased to 20.34 N·m at 25 L/min and 16 N·m at 30 L/min. Excessive gas flow leads to a raise gas porosity in FZ.

For dissimilar weldments, maximum torque was recorded at 200 A, 0.2 second, and 20 L/min. Maximum torque strength recorded for dissimilar is higher than similar weldment. This is due to firstly; Magnesium content in AA5086 is higher than that of AA6061, results in formation of precipitation-hardened (Mg_2Si) phase at FZ, secondly; hot cracks exist with similar ASW weldments, while no cracks with dissimilar weldments appear. Dilution of 6061-T6 by 5086 H116 improves resistance to cracking.

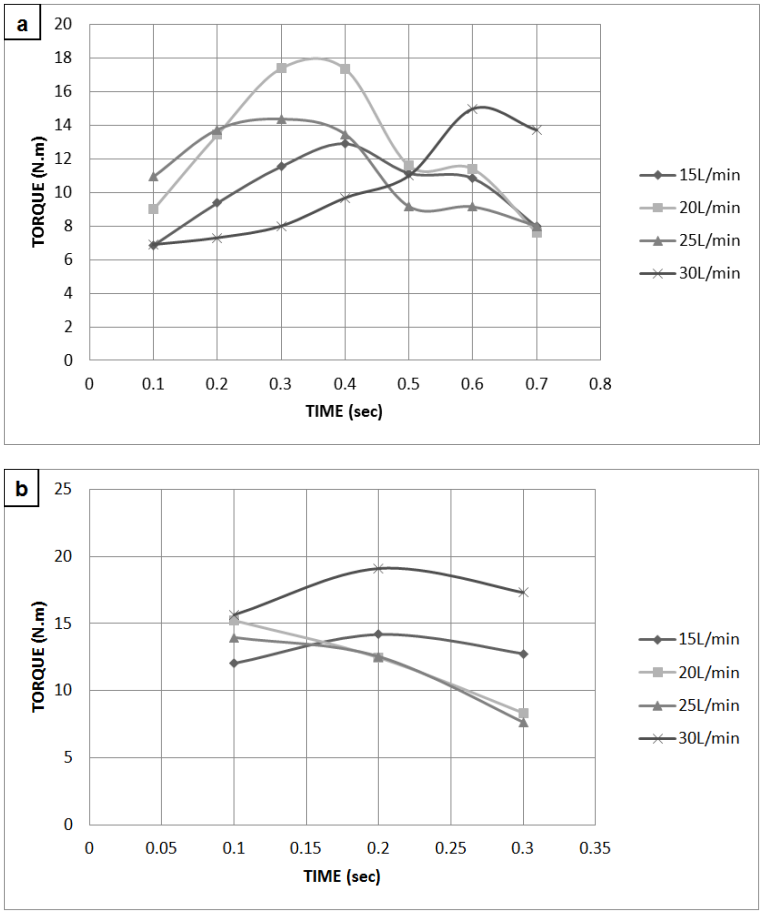

Fig. 9. Torque strength of AA6061-T6/AA6061-T6 weldments at (a) 200A (b) 400A

Torque results showed that optimum welding parameter for similar weldments are completely different from dissimilar weldments, especially for the welding current and welding time, so it is not possible to compare the influence of gas flow rate between similar and dissimilar because of its limited effect corresponding to other variables.

Hardness measurements of AA6061-T6 alloy welds indicated a remarkable softening of FZ due to dissolution of strengthening precipitates, this is confirmed with V. Malin [17]. Hardness profiles through FZ, HAZ, and base metal of similar weldments are shown in Figure 11. Lowest hardness was registered at FZ; then the hardness was increased gradually in HAZ until it became equal to that of BM. Minimum hardness (34 HV) was recorded in FZ at 400 A, 0.2 second, and 30 L/min, which is less 62% than hardness of base metal of AA6061-T6. At the same zone when decreasing current, time, and gas flow rate to 200 A, 0.1 second, and 15 L/min, hardness was increased to 46 HV, that is less 48% than that of base metal. Increasing hardness from welding zone (34 HV) to HAZ (78 HV) can be ascribed to presence of precipitation hardening Mg_2Si and Al_3Mg_2 phases at HAZ. Moving from FZ to BM, effect of welding on strengthening precipitates becomes smaller due to thermal cycling in ASW. Therefore, hardness of BM, HAZ, and FZ of welded joints are BM>HAZ>FZ, this agreed with Dong Peng [18].

For alloy AA5086-H116, softening of HAZ is due to loss of its strain hardening. Maximum hardness (86 HV) was recorded in FZ of dissimilar weldments at 200 A, 0.3 second and 15 L/min – Figure 12. When increasing welding heat input throughout increase welding time to 0.7 second at 200 A and 25 L/min, hardness decreased to 70 HV owing to high heat input that encourages alloying elements like magnesium and silicon to evaporate, which leads to the reduction of mechanical properties [6,19]. Reduction of hardness in similar weldments is larger than that in dissimilar weldments.

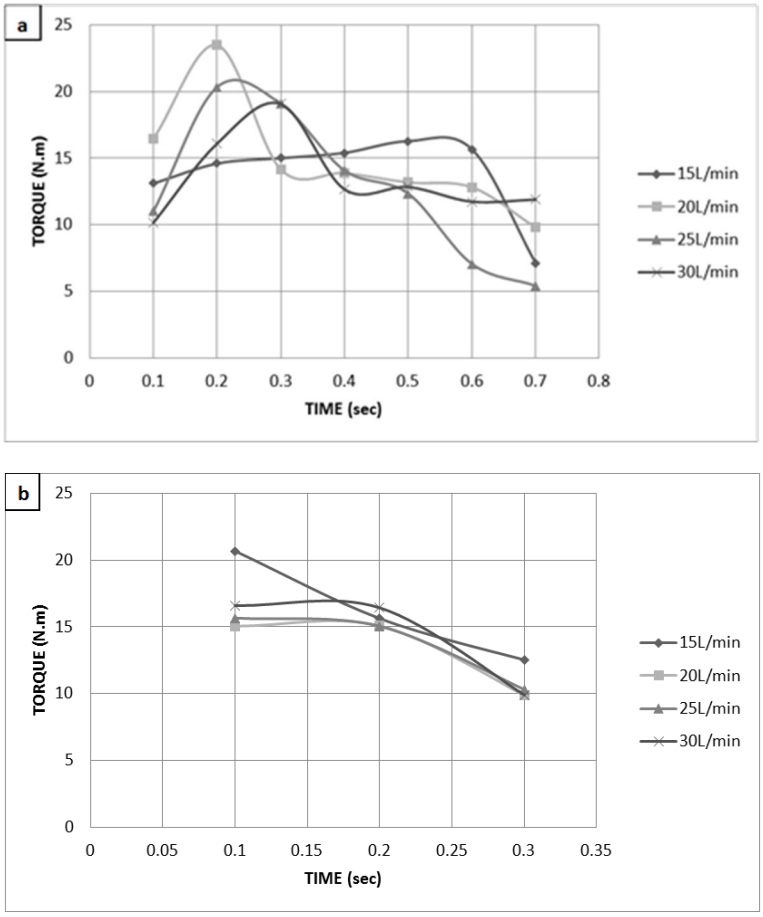

Fig. 10. Torque strength of AA6061-T6/AA5086-H116 weldments at (a) 200A (b) 400A

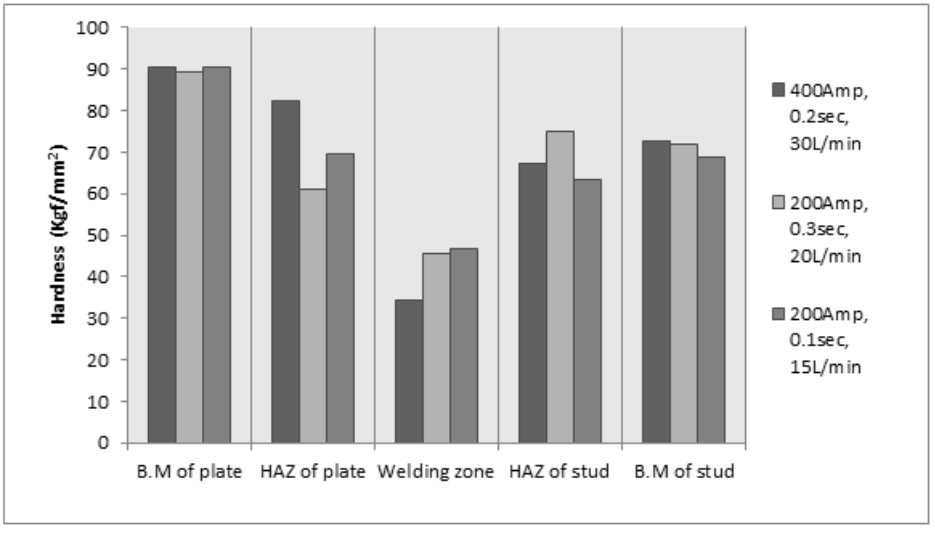

Fig. 11. Hardness across BM, HAZ, and welding zone of AA6061-T6/AA6061-T6 weldments

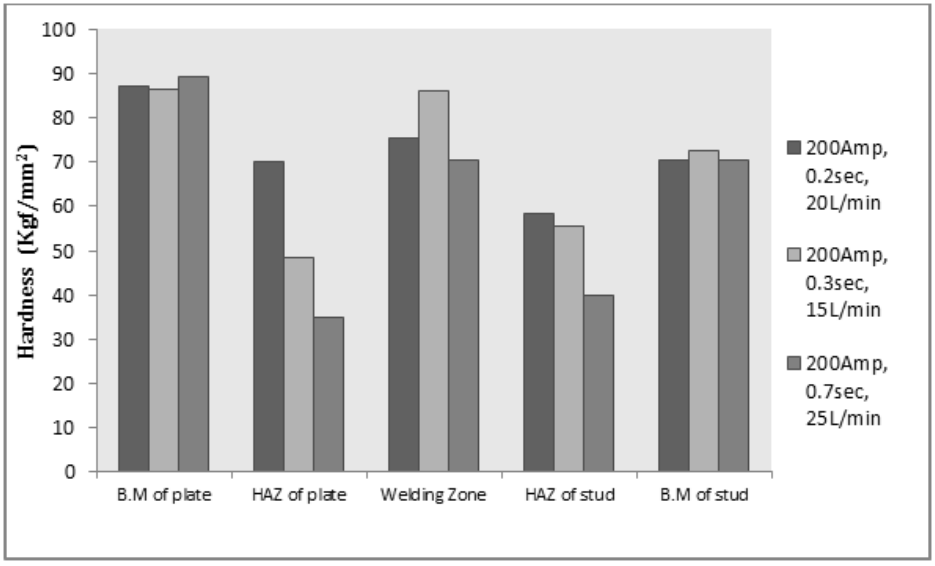

Fig. 12. Hardness across BM, HAZ, and welding zone of AA6061-T6/AA5086-H116 weldments

4. Conclusions

- ASW of AA6061-T6 to stud AA6061-T6 registered maximum torque strength of 19 N·m at 400 A, 0.2 second, 30 L/min.
- For both similar and dissimilar weldments, solidification modes of near the mid of FZ and HAZ are cellular dendritic with equiaxed grains, while at FZ interface, the grains are mainly columnar.
- Lower hardness was registered in FZ for similar weldments and increased toward HAZ and base metal.
- ASW of AA5086-H116 to stud AA6061-T6 recorded maximum torque strength of 23 N·m at 200 A, 0.2 second, 20 L/min.
- Higher hardness was resulted in the FZ for dissimilar weldments and decreased in HAZ.
- Hot cracks exist with similar weldments, while no cracks detect with dissimilar weldments.
- Maximum depth of penetration for dissimilar weldments is higher than that of similar ASW weldments.

References

[1] M.H. Abass, M.S. Alali, W.S. Abbas, A.A. Shehab, Study of solidification behavior and mechanical properties of arc stud welded AISI 316L stainless steel, Journal of Achievements in Materials and Manufacturing Engineering 97/1 (2019) 5-14. DOI: https://doi.org/10.5604/01.3001.0013.7944

[2] E.N. Abbas, S. Omran, M. Alali, M.H. Abass, A.N. Abood, Dissimilar welding of AISI 309 stainless steel to AISI 1020 carbon steel using arc stud welding, Proceedings of the International Conference on Advanced Science and Engineering "ICOASE", Duhok, Iraq, 2018, 462-467. DOI: https://doi.org/10.1109/ICOASE.2018.8548844

[3] H.A. Chambers, Principles and practices of stud welding, PCI Journal 46/5 (2001) 46-59. DOI: https://doi.org/10.15554/pcij.09012001.46.58

[4] Š. Klarić, I. Kladarić, D. Kozak, A. Stoić, Ž. Ivandić, I. Samardžić, The influence of the stud arc welding process parameters on the weld penetration. Scientific Bulletin Series C: Fascicle Mechanics, Tribology, Machine Manufacturing Technology 23 (2009) 79-84.

[5] W. Nishikawa, The principle and application field of stud welding, Welding International 17/9 (2003) 699-705. DOI: https://doi.org/10.1533/wint.2003.3170

[6] B. Wang, S. Xue, C. Ma, J. Wang, Z. Lin, Effects of porosity, heat input and post-weld heat treatment on the microstructure and mechanical properties of TIG-welded joints of AA6082-T6, Metals 7/11 (2017) 463. DOI: https://doi.org/10.3390/met7110463

[7] T. Luijendijk, Welding of dissimilar aluminum alloys, Journal of Materials Processing Technology 103/1 (2000) 29-35. DOI: https://doi.org/10.1016/S0924-0136(00)00415-5

[8] A.B. Başyiğit, A. Kurt, Investigation of the weld properties of dissimilar S32205 duplex stainless steel with AISI 304 steel joints produced by arc stud welding, Metals 7/3 (2017) 77. DOI: https://doi.org/10.3390/met7030077
[9] G. Çam, G. İpekoğlu, Recent developments in joining of aluminum alloys, The International Journal of Advanced Manufacturing Technology 91 (2017) 1851-1866. DOI: https://doi.org/10.1007/s00170-016-9861-0
[10] J. Ion, Laser beam welding of wrought aluminum alloys, Science and Technology of Welding and Joining 5/5 (2000) 265-276. DOI: https://doi.org/10.1179/136217100101538308
[11] A. Karim, Y.-D. Park, A review on welding of dissimilar metals in car body manufacturing, Journal of Welding and Joining 38/1 (2020) 8-23. DOI: https://doi.org/10.5781/JWJ.2020.38.1.1
[12] S. Ramasamy, Drawn arc aluminum stud welding for automotive applications, JOM 54/8 (2002) 44-46.DOI: https://doi.org/10.1007/BF02711866
[13] A. El-Batahgy, M. Kutsuna, Laser beam welding of AA5052, AA5083, and AA6061 aluminum alloys, Advances in Materials Science and Engineering 2009 (2009) 974182. DOI: https://doi.org/10.1155/2009/974182
[14] B. Gungor, E. Kaluc, E. Taban, A. Şik, Mechanical and microstructural properties of robotic Cold Metal Transfer (CMT) welded 5083-H111 and 6082-T651 aluminum alloys. Materials and Design (1980-2015) 54 (2014) 207-211. DOI: https://doi.org/10.1016/j.matdes.2013.08.018
[15] M. Temmar, M. Hadji, T. Sahraoui, Effect of post-weld aging treatment on mechanical properties of Tungsten Inert Gas welded low thickness 7075 aluminum alloy joints, Materials and Design 32/6 (2011) 3532-3536. DOI: https://doi.org/10.1016/j.matdes.2011.02.011
[16] C.W.M. Noor, K. Samo, Nurazilla, M.A. Musa, A.M. Muzathik, The effect of Arc voltage and welding current on mechanical and microstructure properties of 5083-Aluminum Alloy joints used in marine applications, Proceedings of the 10th International Annual Symposium Empowering Science, Technology, and Innovation Towards a Better Tomorrow "UMTAS 2011", Malaysia, 2011,169-178.
[17] V. Malin, Study of metallurgical phenomena in the HAZ of 6061-T6 aluminum welded joints, Welding Research Supplement 74/9 (1995) 305-s-318-s.
[18] D. Peng, P. Dong, J. Shen, Q. Tang, C.-p. Wu, Y.-b. Zhou, Effects of aging treatment and heat input on the microstructures and mechanical properties of TIG-welded 6061-T6 alloy joints, International Journal of Minerals, Metallurgy, and Materials 20/3 (2013) 259-265. DOI: https://doi.org/10.1007/s12613-013-0721-8
[19] K.Vasu, H. Chelladurai, A. Ramaswamy, S. Malarvizhi, V. Balasubraman, Effect of fusion welding processes on tensile properties of armor grade, high thickness, non-heat treatable aluminum alloy joints, Defence Technology 15/3 (2019) 353-362. DOI: https://doi.org/10.1016/j.dt.2018.11.004